Volume 5 Number 1 January 1978 Nucleic Acids Research

Thermal denaturation of nucleosomal core particles

W.O. Weischet, K. Tatchell, K.E. Van Holde and H. Klump*[1]

Department of Biochemistry and Biophysics, Oregon State University, Corvallis, OR 97331 and *Institute of Molecular Biology, University of Oregon, Eugene, OR 97403 USA

Received 30 September 1977

ABSTRACT

Thermal denaturation of very homogeneous preparations of core particles from chicken erythrocyte chromatin is studied by several techniques. The change in absorbance, which is very closely paralleled by changes in heat capacity, is a biphasic process with inflexions at 60°C and 74°C. In contrast, isolated DNA of the same length denatures in a single transition around 44°C. Monitoring the circular dichroism of the cores during thermal denaturation reveals biphasic changes in the secondary structure of the DNA, preceding the base unstacking by 10°C in the first and 3°C in the second phase. However, measurable alterations in the secondary structure of the histones are confined to the second phase with a melting temperature at 71°C. Increase in the ionic strength of the buffer from 1 mM to 10 mM leads to almost monophasic melting curves as measured by absorbance and CD, while not causing any measurable conformational changes at room temperature. The melting of core particles is interpreted as a denaturation of about 40 base pairs in the first phase, followed by a massive breakdown of the native structure of a tight histone-DNA complex, which frees the remaining 100 base pairs for unstacking.

INTRODUCTION

The nucleosomal core particle, containing a 140 base pair length of DNA and two molecules each of the four histones H2A, H2B, H3 and H4, is now recognized to be the fundamental building block of chromatin. Since these structures appear to involve a large fraction of the DNA, including at least some of the transcriptionally active regions of the genome,[2-5] analysis of their structure and conditions for their stability is of the greatest importance. What forces hold them together? Are all portions of the DNA equally tightly bound to the histone core? Under what conditions do the core particles undergo conformational transitions?

Some of these questions can be approached by the simple

technique of thermal denaturation. A number of such studies have appeared, both with "chromatin" prepared in various ways, and with "nucleosomes". However, melting studies on chromatin are complicated by the fact that different regions of the DNA interact with different proteins - some portions with the histone core proteins, some portions with the lysine-rich histones, some portions with non-histone proteins, etc. The behavior of the whole will ultimately have to be understood, but it seems more sensible to first take structural regions of chromatin one at a time.

Several authors have attempted to do this by carrying out thermal denaturation on nucleosome preparations.[6-8] But in all instances such preparations were probably heterogeneous in both DNA size and protein content. We shall show in a subsequent paper (in preparation) that the presence of histone H1 or H5 and the length of the DNA attached to the histone core markedly influence the thermal denaturation behavior.

We have succeeded in eliminating this heterogeneity, using a technique developed by Dr. M. Noll for the preparation of extremely clean core particles.[9] With these particles, we have undertaken studies of the thermal denaturation process, using hyperchromicity, circular dichroism and calorimetry as experimental techniques. The results reveal new information about the DNA-protein interactions in these particles.

MATERIALS AND METHODS

A. Preparation and digestion of histone H1 and H5 depleted chromatin. Chicken erythrocyte nuclei were prepared exactly as described in a recent publication.[10] Freshly prepared nuclei from 6 ml packed erythrocytes were lysed in 250 ml of 10 mM Tris-cacodylic acid, pH 7.2, 0.7 mM EDTA, 0.1 mM PMSF (lysis buffer), then made 0.6 M NaCl with solid NaCl and allowed to swell overnight at 4°C. The chromatin gel was transferred to 250 ml lysis buffer containing 0.65 M NaCl and allowed to stand for 24 hr with gentle stirring. It was then centrifuged at 17,000 x g for 30 min. The pellet was brought up in 250 ml of lysis buffer and stirred for 4-8 hr. The chromatin was centrifuged at 17,000 x g for 30 min, brought up in 10-15 ml

lysis buffer (with 1 mM $CaCl_2$ replacing EDTA) and digested at 37°C with 125 units/ml micrococcal nuclease (Worthington). The reaction was terminated after 60 min by making the solution 10 mM in EDTA and cooling on ice. The acid solubility of the DNA was 27% at this point.

B. Preparation of core particles from digested chromatin. Core particles were isolated from chromatin digests by the method of Shaw et al.[11] using gel chromatography on Biogel A5m. Peak fractions were run on isokinetic sucrose gradients (5-26.9%)[12] (Beckman SW40) to separate the core particles from a small amount of dimeric nucleosomes. In some preparations, the initial A5m column separation was replaced by sucrose gradient centrifugation.

C. Thermal denaturation. Since EDTA has been reported to alter chromatin structure[13-15] we performed all melting experiments in cacodylate buffer of low ionic strength instead of the buffer most commonly used in this type of investigations (0.25 mM EDTA at pH 8.0). Core particles for thermal denaturation studies were dialyzed extensively against 1.0 mM cacodylate buffer, pH 7.2. Samples with 0.5-1 A_{260} were placed in quartz cuvettes with 1 cm pathlength, bubbled with helium to de-gas the solution, then overlayered with Dow Corning 200 silicone fluid and sealed with ground glass stoppers. Absorbances and temperatures were recorded directly on punch tape from a Beckman Acta III spectrophotometer. The temperature readings of the Acta III probe were calibrated against a themister probe placed directly in the sample cuvette. The rate of temperature increase was 0.25°C/min and one set of data (absorbance, reference absorbance, and temperature) was collected every minute. The data were processed with a Hewlett Packard 9521 minicomputer, correcting for thermal expansion, to give percent hyperchromicity (h) vs. temperature (T) or the first derivative of h with respect to T. The percent hyperchromicity at temperature T is defined as:

$$h = \frac{A_{260} - A^{\circ}_{260}}{A^{\circ}_{260}} \times 100$$

where A_{260} is the absorbance at T, (corrected for thermal expansion) and A°_{260} the absorbance at the base temperature (usually 20°C). A linear least squares fit in an interval around each

point in the curve was used to obtain the derivative dh/dT. We have varied the width of the interval from 1.8° to 7°C and have found no effect on the peak positions which we define as melting temperatures.

D. Calorimetric measurements. Calorimetric measurements were performed with an adiabatic differential scanning calorimeter, Type DASM, constructed by the Institute of Protein Research of the Soviet Academy of Sciences. The sample chamber was filled with 1.0 ml solution of core particles in 1.0 mM cacodylate buffer pH 7.2 (melting buffer) at a concentration of 0.5-2.0 mg/ml. The same amount of buffer was placed in the reference chamber; the chambers were then de-gassed, sealed, and an additional pressure of 1 kg/cm^2 was applied to them.

The sample and blank were heated at a constant rate of 0.5 or 1.0 deg/min. The output signal, which is proportional to the energy required to keep the temperature difference of the two cells close to zero, was recorded as a function of temperature. Conformational changes of the dissolved biopolymers are shown as peaks on a baseline. During each run an external electronic signal is used to put a calibration peak on the recorder tracing. The total enthalpy change (ΔH_{cal}) due to an order-disorder transition of the biopolymer can be calculated by comparing the experimental peak area with the area of the calibration peak.

E. Circular dichroism. The CD spectra of the core particle preparations were recorded with a Jasco J-41A spectropolarimeter calibrated against camphor-sulfonic acid. We used a jacketed cylindrical cuvette with 1 cm optical pathlength. Temperatures were recorded with a thermister directly immersed in the sample. The cell was stoppered to prevent evaporation. Samples were prepared as described under section C. We performed two types of experiments: 1. Spectra were recorded between 200 and 260 nm and 250 and 330 nm at a constant temperature, followed by a baseline scan with buffer at the same temperature. 2. The melting of a sample was monitored at a fixed wavelength (λ = 223 nm; λ = 273 nm) while the temperature was linearly increased by about 0.2 deg/min. In these cases buffer baselines were recorded at the initial and final temperatures only. The recorder

graphs were digitized and converted to mean residue ellipticities, Θ, or changes thereof, $\Delta\Theta/\Delta T$, using an extinction coefficient of 6600 per mole of nucleotide residue at room temperature.

RESULTS

1. Quality of the core particle preparations. We define a chromatin "core particle" as containing within a few base pairs of 140 base pairs of DNA and only the four histones H2A, H2B, H3 and H4. Such particles are homogeneous in the ultracentrifuge, with $S^{\circ}_{20,w}$ = 11.0 ± 0.2 S.

An integral distribution of sedimentation coefficients[16] of the preparations used in this study shows that virtually all the material sediments between 10.8 S and 11.2 S. Gel electrophoresis of the DNA extracted from these particles[10] is shown in Figure 1 (Top). The size of the DNA, as judged by comparison with HaeIII-restriction fragments of PM2 DNA,[17] is 139 bp. Its size distribution is skewed and the half width of the DNA band is + 12 - 3 bp. This is certainly an overestimate of the breadth, for it has not been corrected for diffusion in the gel and finite initial band width. Contamination by other DNA sizes is less than 5%, as judged by such scans. Examination of such DNA on denaturing gels shows no evidence for single strand nicks.

The protein composition of the core particles can be seen on the SDS gel[18] shown in Figure 1 (Bottom). The only proteins present in significant amounts are H2A, H2B, H3 and H4 and they are found in apparently equal quantities. No protein can be seen at the positions expected for H1 and H5, nor are significant quantities of non-histone proteins detectable.

Thus, the particles used in the experiments described below are homogeneous and of simple, defined composition.

2. The thermal denaturation, as followed by hyperchromicity measurements, is a reproduceable, biphasic process. Three points should be emphasized. First, such data are reproduceable in detail from preparation to preparation and even in reconstituted particles. As has been shown elsewhere, the derivative melting curve obtained with reconstituted particles is virtually identi-

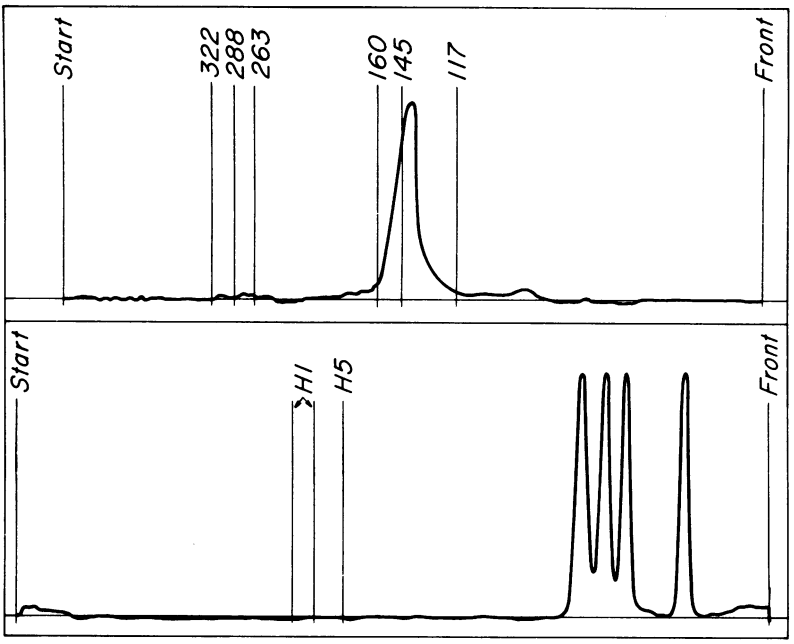

Figure 1 Top: Scan of the core-DNA on a 6% polyacrylamide gel stained with ethidium bromide. The markers correspond to co-electrophoresed PM2-HaeIII-fragments. Bottom: SDS-gel of the core-histones. The positions of the H1- and H5 bands stem from co-electrophoresis of total erythrocyte histones.

cal with that for the native particles.[10] This means that this curve is the result of a particular kind of spontaneous DNA-protein interaction and is not an artifact of preparation.

Second, as can be seen in Figure 2 (Top) the curve is unquestionably biphasic. In early experiments, with inhomogeneous particle preparations, we thought that biphasic curves resulted from heterogeneity. We then were surprised to find a reproduceable, biphasic melting curve for what are clearly homogeneous particles. Thus, the biphasic form of the curve must reflect features of the internal structure of the core particle.

Third, up to a point, the thermal denaturation is reversible. If one raises the temperature to 62°C, at which point the first phase of the transition is largely complete, and then reduces the temperature, the original absorbance is regained and a second melt is indistinguishable from the first. On the other

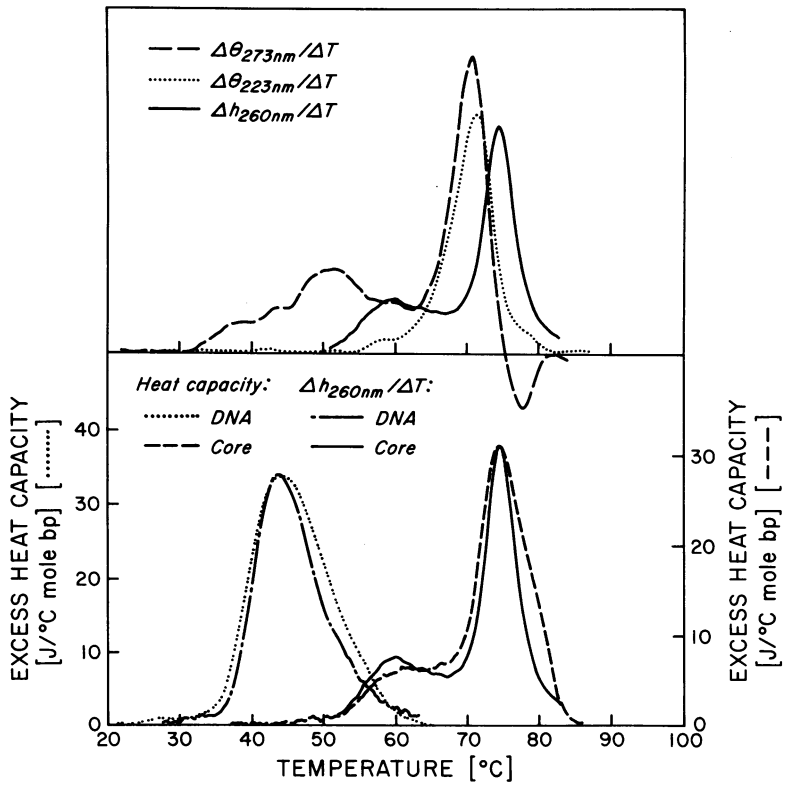

Figure 2 Top: Comparison of the derivative melting curves of core particles as followed by CD at two wavelengths and hyperchromicity. Bottom: Comparison of heat capacity measurements and derivative hyperchromicity melting curves for isolated core DNA and core particles.

hand, if the heating is continued to the midpoint of the second transition (~74°C) evidence for irreversible changes (incomplete decrease of absorbance) is found upon cooling. Thus, the two stages in the transition can be distinguished in this way.

3. Different conformational changes of the protein and DNA are found during thermal denaturation. We next ask, do both stages of the melting involve both protein and DNA, or are they distinguishable in this repect? To examine this question, we used circular dichroism measurements. Figure 3 (Top) displays CD spectra of core particles (in two wavelength ranges) obtained at different temperatures. The CD at wavelengths above 250 nm is

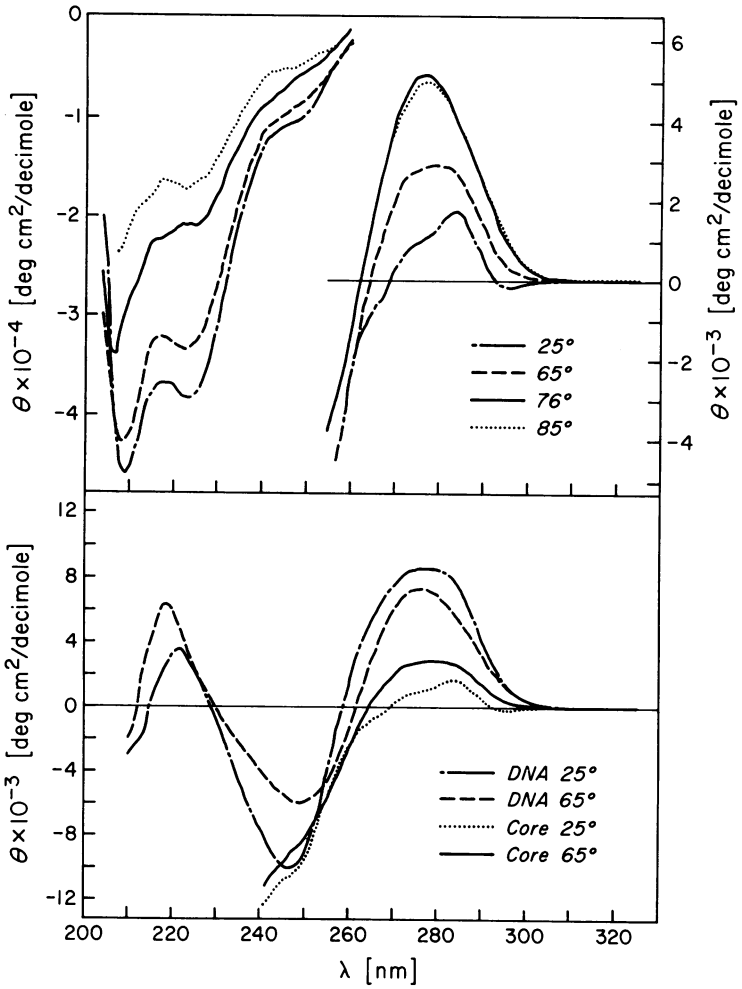

Figure 3: CD-spectra of core particles (Top) and core DNA (Bottom) at different temperatures as indicated.

almost entirely due to the DNA[19-21] and is strongly affected by its conformational changes.[22] At lower wavelengths both DNA and proteins contribute[23] but the DNA contribution is minimal.[22,24] Moreover, the CD of the DNA in chromatin below 250 nm has been reported to be the same as that of DNA in solution at low ionic strength.[23] Since the DNA-CD around 220 nm is little affected by melting,[25] (cf. Figure 3 (Bottom)) the relative contributions of histones and DNA to the overall CD spectrum of the core particles can be estimated at all temperatures from Figure 3.

Inspection of Figure 3 shows that increasing temperature shifts the spectrum above 250 nm towards that of free, B-form DNA. But neither is a typical B-form spectrum obtained transiently nor are the spectra of denatured core particles ($\geq$ 85°C) and denatured DNA ($\geq$ 65°C) the same. The latter may indicate that the histones still bind to the denatured DNA strands.

Below 250 nm the CD spectra show a decrease in amplitude with increasing temperature. In particular, the minima at 208 nm and ~225 nm disappear or are blue-shifted. The same findings with chromatin have been interpreted as indicative of the loss of secondary structure in the histones.[22,24] In an attempt to quantitize this statement we calculated the proportions of peptide secondary structures in both native and heat denatured cores by the method of Baker and Isenberg.[26] Tentative histone spectra between 210 and 240 nm were constructed by subtracting the DNA spectrum at 25° from that of the cores at 25°C or the DNA spectrum at 65° from the core spectrum at 76°C (cf. Figure 3). The latter correction will include some error from a possible temperature-dependence of the spectrum of denatured DNA, but otherwise these corrections should be permissible according to the above mentioned reports.

For the native condition the results are 40% α-helix, 0% β-structure and 50% random coil. These numbers are independent of the choice of reference spectra (either from Greenfield and Fasman[27] or from Chen *et al.*[28]) and of the wavelength range chosen for evaluation. For the denatured spectrum we derive 16% α-helix, 20% β-structure and 40-70% random coil using poly-L-lysine reference spectra,[27] or 26% α-helix, 10% β-structure and 50-90% random coil, using Chen's spectra.[28] The results are not strongly influenced by choosing a wavelength range for analysis. This is one criterion for reliability of the calculations, another being that the three fractions sum up to ~100%.

A source of error which will contribute to an unknown extent, is the uncertainty in choice of a suitable reference spectrum for the random conformation of histones. This has been emphasized before[26] when spectra of acid denatured histones were used as references. However, evaluating the tentative secondary structure of the histone octamer within the

core particle we found a reference of acid denatured H1 or stoichiometrically mixed H2a, H2b, H3, H4 unsatisfactory, since those results generally did not meet the sum condition.

Examining Figure 3, we note that large CD changes are observed at 273 nm and 223 nm. The former will measure DNA conformational changes, the latter, because the DNA contribution is small and probably invariant with temperature, will primarily follow histone rearrangements. Therefore we chose to follow the ellipticity changes at 223 nm and 273 nm continuously through the melting range. The most striking result of this study, shown in Figure 2 (Top) is the monophasic melting curve observed for the CD at 223 nm, the lower temperature transition being completely absent. In contrast, the curve monitored at 273 nm resembles the absorbance melting curve, but is shifted to lower temperatures. This is apparently true for both the premelt and the main peak. A comparison between the spectra in Figure 3 and the change in ellipticity in Figure 2 indicates that the typical long wavelength CD spectrum of core particles, which involves a negative band at about 295 nm and a "doublet" peak in the range between 270 and 290 nm, is lost first. This seems to be half completed at 50°C where the melting of a part of the DNA starts. At 65°C a stage is reached where no evidence for these spectral features is left. The fraction of the DNA denatured at this point amounts to about 27%, as calculated from the area under the derivative hyperchromicity curve. The conformation of the histones, as judged by CD, has still changed only very little if at all. Above 65°C the signals at both 223 nm and 273 nm change almost simultaneously yielding melting temperatures of 71.3°C and 70.7°C, respectively. The corresponding maximum in the derivative plot for the hyperchromicity signal is observed more than 3° higher. A similar difference (about 4°) has been observed by Mandel and Fasman.[7] The close resemblence of the change in the CD signal at 273 nm and in the absorbance signal suggests that we are monitoring different effects involving the same part of the DNA during the premelt in each case. However, since the nature of the CD changes in either the premelt or the main transition are different, it is not expected that the proportions of the areas under the de-

rivative curve are the same as calculated from hyperchromicity.

4. Thermodynamics of the thermal denaturation. There are two general ways in which a thermodynamic analysis of such a process can be approached. The first is to calculate the van't Hoff enthalpy from the relationship

$$\frac{\partial \ln K}{\partial (1/T)} = - \frac{\Delta H^{\circ}_{vH}}{R}$$

Such an analysis is only strictly justified if the transition is a two-state process. Furthermore, the change in the physical property used to follow the reaction must be directly proportional to the extent of the reaction.

A more direct analysis can be made using calorimetry. In this case, the enthalpy change is measured directly and no assumptions regarding the nature of the process are involved. Nevertheless, the combination of the two approaches provides valuable additional information. In the thermal denaturation of a polymer like DNA, the ratio of the van't Hoff and calorimetric enthalpies gives a measure of the size of the cooperative unit in the denaturation process.

To derive the van't Hoff enthalpy data from spectroscopic data, the experimental curves have to be replotted in terms of the fractional change in the quantity measured (absorbance in this case) versus temperature.[29] In a similar way, the calorimetric data can be used to calculate ΔH_{vH} (cf. Figure 4) in addition to ΔH_{cal}.

We first describe studies with DNA obtained from core particles. Figure 2 (Bottom) shows the plot of the compensating energy as a function of the temperature for DNA. The peak is asymmetric, with the slope at the high temperature side being slightly smaller. This is possibly due to the presence of a small fraction of DNA strands longer than the average 139 base pairs (cf. Figure 1 (Top)).

The curve due to the thermally induced transition of the core particles is entirely different from the one for DNA (cf. Figure 2 (Bottom)). Heat compensation starts at 51°, reaches a plateau at 61° and increases to a second maximum at 74.3°C. The baseline after the transition is reattained at around 85°C. There is a pronounced shoulder on the high temperature side of

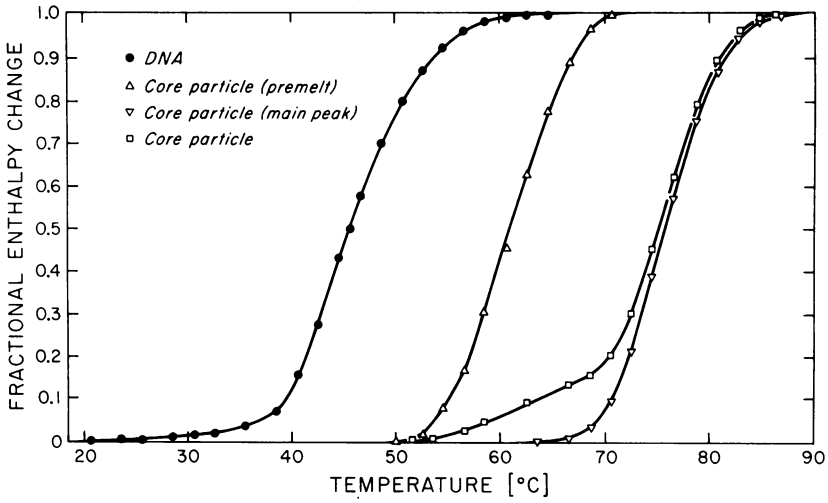

Figure 4: Plot of the degree of transition vs. temperature for core DNA (o——o), premelt (Δ——Δ), main transition (∇——∇) and total melt of core particles (□——□). The curves were constructed from the calorimetric data in Figure 2.

the higher peak centered at about 80°C.

Repeating a run with the same sample results in a straight line if the temperature of the second maximum was surpassed in the first run, showing that the thermal denaturation is irreversible above 74°C. In contrast, if the sample is first heated to only 64°C and subsequently cooled to room temperature, a second heating is exactly like that observed for samples that had not been previously heated. This reversibility for the first transition confirms the result from hyperchromicity (see above).

The thermal transition appears to be independent of the particle concentration: We ran a set of experiments changing the concentration from 0.43 to 1.7 x 10^{-6} mole base pairs/L but could not detect any difference due either to concentration or sample preparation.

5. Dependence of thermal denaturation on ionic strength. Hyperchromicity melting experiments were repeated in tenfold more concentrated and tenfold more dilute buffer than in the above experiments. A solution of core particles ($A_{260} \approx 9$) in 1 mM cacodylate, pH 7.2 was diluted 1:16 fold into 0.05 mM cacodylate or 10 mM cacodylate of the same pH. Thus, the exact

final buffer concentrations were 0.11 mM and 9.44 mM, respectively; we will refer to them as 0.1 and 10 mM. The derivative melting curves are shown in Figure 5. The sample in 10 mM cacodylate begins to aggregate at around 79°C as shown by light scattering at 340 nm.

To a first approximation, the main transition seems to be shifted linearly with the logarithm of the buffer concentrations. The melting temperatures are 71.0°, 74.4°, ~78°C for 0.1 mM, 1.0 mM, 10 mM cacodylate, respectively (cf. Table I). Thus, the shift is only half that reported for different chromatins.[30] In contrast, the premelting undergoes a much larger and non-linear shift. In fact, the premelt, which is well resolved at low ionic strength, is transformed by 10 mM cacodylate to a broad shoulder of the main melting transition.

We also followed the thermal denaturation in 10 mM cacodylate by measuring the ellipticity at 273 nm (data not shown).

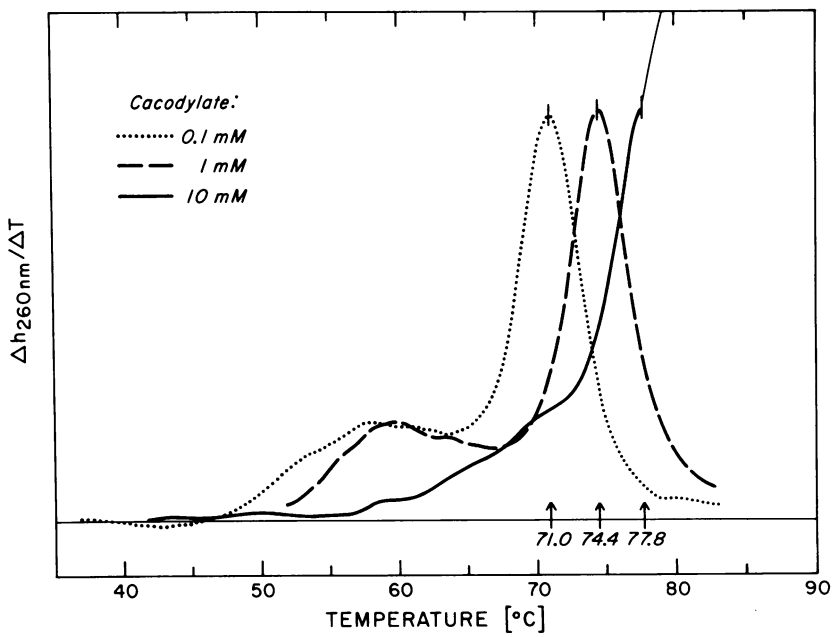

Figure 5: Effect of ionic strength on the melting of core particles. Shown are the derivatives of hyperchromicity curves followed at 260 nm at the various buffer concentrations indicated. The onset of aggregation at 79° in 10 mM cacodylate is indicated by the change in line thickness.

As in the case of the experiments in 1 mM cacodylate the CD-signal resembles the hyperchromicity curve but precedes it, in this case by about 8°C. The important fact is that the CD change, like the hyperchromicity, does not show a well resolved premelt at this ionic strength.

Why does the shape of the melting curve change upon increase in ionic strength? It is conceivable that either the DNA or the histones assume a different conformation at the higher ionic strength which allows more mutual stabilization. If such changes involve the secondary structure of the protein or DNA,

	Transition Temperature	
Core Particle:	Premelt [°C]	Main Peak [°C]
1 mM cacodylate		
Absorbance 260 nm	60.0 ± 5.3	74.4 ± 2.6
CD 273 nm	50.0	70.7 + 2.3 - 3.5
CD 223 nm	-	71.3 + 2.6 - 3.8
Heat capacity	~61	74.3
0.1 mM cacodylate		
Absorbance 260 nm	57.7 ± 6.0	71.0 ± 2.8
10 mM cacodylate		
Absorbance 260 nm	~70.0	~78
DNA:		
1 mM cacodylate		
Absorbance 260 nm	-	44.1
Heat capacity	-	44.2

Table I: Summary of the melting temperatures of core particles and DNA in different ionic strengths. Shown are peak positions and half-widths, where measurable, of derivative curves obtained by absorbance or CD-measurements.

they should be detectable from changes in the room temperature CD spectra. In the near UV, a comparison of the core particle spectrum in Figure 3 with spectra recorded in 10 mM Tris-HCl, 0.7 mM EDTA, pH 7.4 shows no difference within the margin of accuracy, i.e., ± 2-3% (data not shown). Recording the far UV part of the CD spectrum below 250 nm in the buffers and at nucleosome concentrations used for the melting experiments yields equally superimposable scans.

DISCUSSION

The thermal denaturation of the core particles is a reproducible two step process. Biphasic melting curves very similar to

the one in Figure 2 were reported by Mandel and Fasman.[7] But apart from these results, mononucleosomes have been described[6,8,31,32] as having monophasic melts with a melting temperature consistently higher than the value of 74°C observed here (cf. Table I). We believe that these discrepancies result from different methods of sample preparations and/or the presence of H1 in the mononucleosomes. Both a recent report[10] and preliminary experiments in this laboratory indicate that in the presence of H1 the two transitions are shifted together and raised to about 80°C. A wider length distribution of the core DNA has a similar effect.

The first step in the thermal denaturation of core particles is a conformational change in about 30-40 bp of the DNA. This process, monitored by an increasing ellipticity at 273 nm, starts between 30° and 40° and reaches its midpoint at 50°C (cf. Figure 2). The change is such that this portion of the DNA adopts a CD spectrum more like that of the B-form. The actual base unstacking of this part of the DNA follows with a melting temperature at around 60°C.

It is tempting, although not rigorously justified to correlate the early melting part of the DNA with some bases which are in a C-form conformation in the native state. In fact, this has both been done[24] and contradicted before.[33] Since the amplitude of the CD spectrum around 280 nm after the premelting is still less than half that of native DNA it must be concluded that the bases remaining stacked have not yet assumed a normal B-form conformation.

It is important to note that circular dichroism does not give evidence for any change in secondary structure of the histones accompanying this portion of the DNA melting. Apparently the thermally stable protein core locks the major part of the DNA in a rigid complex allowing only certain regions to gain limited mobility at around 50-60°C. The retention, at this temperature, of a center of native structure explains the complete reversibility of the first melting transition. Thus, there are grounds to speculate that the regions involved in this first melting step are the ends of the DNA coil. This interpretation is consistent with the recent observation[34] that the first regions to be tightly bound to the core are 20-35 residues

from either 5' end. However, other interpretations cannot be excluded at this date.

In contrast, the second and main melting transition seems to be initiated by a massive disruption of the secondary structure of the proteins, accompanied by a change in the DNA conformation. We consider this one overall process and not, like earlier interpretations[24] a conformational change in the proteins followed by another conformational change in the DNA. From the width of the transition one concludes that it must be highly cooperative. It is believed that most of the secondary structure of the histones is located in the more hydrophobic domains[35,36] which are also the parts which interact with each other.[37] We therefore conclude that the CD transition at 223 nm actually monitors the destruction of the histone core at about 70°C. Coupled with it is a relaxation of conformation constraints on the DNA. One possible explanation for the observed changes is that once the histone-histone interactions are disrupted, the DNA can extend from the supercoiled state and adopt a conformation more like that found in dilute solution. Only in such a relaxed DNA conformation can the base unstacking occur which is subsequently manifested as an increase in absorbance. This final denaturation seems to involve all of the remaining 73% of the DNA (about 100 bp). The conformational changes in both the histone core and the DNA are a necessary prelude to the subsequent base unstacking. This seems reasonable regarding the fact that at different buffer concentrations the shape of both the absorbance and the CD melting curve is altered similarly while the temperature displacement between them remains.

As has been pointed out by Mandel and Fasman[7] the final melting step consists of two processes which have very different effects on the CD spectrum: the relaxation of the DNA conformation which yields an increase in ellipticity and the subsequent melting of the DNA duplex accompanied by a decrease in ellipticity. This may be the explanation for the overshoot in the change of ellipticity at 273 nm at 76°C (cf. Figure 2 (Top) and why the ellipticity never reaches at intermediate temperatures the value expected for B-form DNA (cf. Figure 3).

Since our figures about the amount of secondary structure

in the histones will be compared to some recent reports[38-40] they deserve a comment. First they are in reasonable agreement with the values obtained by different and independent techniques of Raman spectroscopy.[38] Our calculations contain two kinds of errors. The first arises from the correction for the DNA contribution to the overall CD spectrum of core particles. The second kind is implied in the method of analysing spectra. Only for these latter errors do we have a quantitative way of estimating the quality of the calculations. As pointed out by Baker and Isenberg[26] the calculated relative amounts of α, β and random structure must be positive, sum up reasonably close to 100% and be independent of the wavelength range used. These conditions are met for our calculation. The results for the native particles do not depend on the choice of reference spectra, which lends support to these values. This is not so for the denatured cores. Although the internal criteria for applicability are also met here, the results are quite different depending on whether poly-lysine data[27] or protein data[28] are used as reference spectra. For this reason, it seems premature to draw conclusions from the apparent increase in β-structure in the cores upon melting. It should be noted, however, that Thomas et al.[38] also find a loss in α-helix and increase in β-structure upon thermal denaturation of protein cores.

Support for the above picture of the thermal denaturation and additional information about the processes involved come from the calorimetric studies. The transition enthalpy obtained for the isolated 140 bp DNA from chicken erythrocyte fits very well into the results obtained for different DNAs from prokaryotes or eukaryotes.[41] The melting temperature (cf. Table II) is also in agreement with the data reported by Privalov et al. for the denaturation of phage DNA as a function of the ionic strength.[42] The approximately symmetric peak observed in the calorimetric study of DNA melting (Fig. 2, bottom) suggests that the melting starts predominantly from the ends. Any melting from occasional loops would lead to a steeper slope on the high temperature side.[43] Since the peak shows just the opposite shape, it is reasonable to assume that, at a chain length of 140 base pairs, loop formation during melting is improbable. This

is in agreement with theoretical calculations.[44]

The calorimetric melting curve of the core particles shows an entirely different shape. There is a pronounced and fully reversible premelting before the main process. Noting the strong resemblence between the curves measured by calorimetry and absorbance, we interpret the premelting transition as originating from the same part of the DNA in both cases. Furthermore the enthalpy change in the premelt region must result mainly from DNA changes, since measurable thermal effects in the histones start only at 60°C (cf. Figure 2). Thus, the area under

	T_m a) [°C]	ΔH_{cal} b)	ΔS c)	$\Delta G°$ b)	ΔH_{vH} d)	$\frac{\Delta H_{vH}}{\Delta H_{cal}}$
DNA	45.5	6.59	20.6	0.45	81	12.3
premelting	61.0	7.50	22.4	0.84	106	14.2
melting	76.0	12.15	34.8	1.79	128	10.5

Table II: Thermodyanmic parameters for the thermal denaturation of core particles and isolated core DNA. a) T_m calculated from the midpoints of the transition curves shown in Figure 4; b) in Kcal/mole base pairs; c) in entropy units/mole base pairs; d) calculated from the curves in Figure 4.

the melting curve for the core particles can be divided into two separate peaks assuming a nearly symmetrical premelt similar to the one observed with hyperchromicity. This means that any calorimetric contributions from conformational changes of the histones must reside in the main peak. As shown above from the hyperchromicity melting curve the fraction of the DNA involved in the premelting can be determined to be 26.5% of the total DNA. Hence, the transition enthalpy calculated for this part of the DNA is 7.5 Kcal/mole base pairs. This value is in good agreement with the ones obtained for native DNA in other investigations.[45] Thus, the thermodynamic behavior of this fraction of the DNA can be hardly affected by the protein associated with the neighboring DNA. Furthermore, the cooperative length is equal to the cooperative length of isolated DNA within the margin of experimental error (cf. Table II).

However, it is important to note that the DNA conformational change that precedes the premelt transition (at about 50°C, see

Figure 2 (Top)) has no counterpart in the calorimetric melting curve. This means that this conformational change, whatever it may be, does not involve a significant enthalpy change.

The calculation of the transition enthalpy for the fraction of DNA involved in the main transition is complicated by the fact that the histone denaturation also contributes to this denaturation enthalpy. A comparison between the appropriate curves in Figure 2 shows that the change of the secondary structure of the histones falls into the temperature range covered by the second transition in the excess heat capacity. Also the shoulder on the high temperature side of the calorimetric data cannot be correlated with the optical data of the DNA denaturation and may therefore indicate some contribution from the proteins. We are thus forced to consider a limiting case. If we assume that the contribution of the histones is negligible, the transition enthalpy of the DNA amounts to 12.2 Kcal/mole base pairs. This value is much larger than the one obtained for native DNA and the assumption seems to be invalid. If, however, one compares this value with the results recently published for the total heat of denaturation of DNA fully associated with poly-L-lysine[45] it fits very well. A result of 12.2 Kcal/mole base pair has been obtained for a complex with a lysine:nucleotide phosphate ratio of 0.66:1.0. Applying the model of overlapping binding sites[46,47] one can calculate that at this ratio the maximum coverage of the DNA is almost reached.

Even though the calorimetric denaturation curve shows subtle differences in shape from the hyperchromicity curve, any attempt to resolve this curve into "protein" and "DNA" components would be hazardous. We must content ourselves with the statement that the value of 12.2 Kcal/mole base pair undoubtably represents a maximum value for the heat of denaturation of this part of the DNA.

Using the above described procedure to separate the premelt and the main transition allows us also to calculate ΔH_{vH} for the two different fractions of the DNA and thereby the cooperative lengths. As shown in Table II, the two values agree quite well, especially when regarding the fact that ΔH for the main transi-

tion is likely to be overestimated due to the unresolved protein contributions. Within the margin of error they are the same as the value found for DNA alone. This indicates that the cooperativity of the melting process is essentially the same in the melting regions of the core particles as in free DNA. However, since there appear to be conformational transitions preceding both melting ranges of the particles, we cannot conclude that the structure of DNA in the native particles is the same as in solution.

The order of events described above is similar to the one proposed earlier[24] from experiments with solubilized chromatin. There is, however, an important difference in that we are dealing with a simple, well defined and very homogeneous system devoid of any interaction between core particles. In our opinion only this fact makes it feasible to correlate the various processes observed by different methods with each other. As an illustration let us reconsider the effect of increasing ionic strength on the melting profile. If, as proposed above, the presence of histone H1 exerts a similar shift in T_m as does an increase in ionic strength, some results from earlier investigations become understandable. Mononucleosomes with a stoichiometric complement of H1 show only one melting transition.[8] This has led to the proposition of a homogeneous interaction between DNA and histones in mononucleosomes.[8] Our results clearly contradict this idea in that they reveal at least two kinds of interactions.

ACKNOWLEDGEMENTS

We wish to acknowledge the expert technical assistance of Ms. G. Riedel and M.H. Carroll and the help of S. Ballard in preparing the manuscript. Dr. E. Small and S. Weber provided CD-reference spectra of denatured histones and Dr. J. Cardenas made an interfaced spectrophotometer accessible to us. This research was supported in part by Grants from the American Cancer Society (NP 201), the National Science Foundation (PCM 7523461) and the National Institutes of Health (GM 22916). Two of us (HK and WOW) were supported by the Deutsche Forschungsgemeinschaft. KVH wishes to acknowledge the support of an American Cancer Society Research Professorship.

REFERENCES

1 Permanent Address: Institut fuer physikalische Chemie der Universitaet Freiburg (GFR).

2 Lacy, E. and Axel, R. (1975) Proc. Natl. Acad. Sci. USA 72, 3978-3982.
3 Laird, C.D., Wilkinson, L.E., Foe, V.E. and Chooi, W.Y. (1976) Chromosoma 58, 169-192.
4 Gottesfeld, J.M., Bagi, G., Berg, B. and Bonner, J. (1976) Biochemistry, 15, 2472-2483.
5 Kuo, M.T., Sahasrabuddhe, C.G. and Saunders, G.F. (1976) Proc. Natl. Acad. Sci. USA 73, 1572-1575.
6 Woodcock, C.L.F. and Frado, L.L.Y (1975) Biochem. Biophys. Res. Commun. 66, 403-410.
7 Mandel, R. and Fasman, G.D. (1976) Nucl. Acids. Res. 3, 1839-1855.
8 Lawrence, J.-J., Chan, D.C.F. and Piette, L.H. (1976) Nucl. Acids Res. 3, 2879-2893.
9 Noll, M. (1976) in Organization and Expression of Chromosomes, Dahlem Konferenzen, Berlin, pp. 239-252.
10 Tatchell, K. and Van Holde, K.E. (1977) Biochemistry, in press.
11 Shaw, B.R., Herman, T.M., Kovacic, R.T., Beaudreau, G.S. and Van Holde, K.E. (1976) Proc. Natl. Acad. Sci. USA 73, 505-509.
12 McCarty, K.S., Jr., Vollmer, R.T. and McCarty, K.S. (1974) Anal. Biochem. 61, 165-183.
13 Williams, R.E., Lurquin, P.F. and Seligy, V.L. (1972) Eur. J. Biochem. 29, 426-432.
14 Johnson, R.S., Chan, A. and Hanlon, S. (1972) Biochemistry 11, 4347-4358.
15 Reeck, G.R. (1976) Arch. Biochem. Biophys. 172, 117-122.
16 Van Holde, K.E. and Weischet, W.O. (1977) Biopolymers, (in press).
17 Kovacic, R.T. and Van Holde, K.E. (1977) Biochemistry 16, 1490-1498.
18 Laemmli, U.E. (1970) Nature 227, 680-685.
19 Simpson, R.T. and Sober, H.A. (1970) Biochemistry 9, 3103-3109.
20 Permogorov, V.I., Debabov, V.G., Sladkova, I.A. and Rebentish, B.A. (1970) Biochim. Biophys. Acta 199, 556-558.
21 Fasman, G.D., Scharffhausen, B., Goldsmith, L. and Adler, A. (1970) Biochemistry 9, 2814-2822.
22 Li, H.J., Chang, C., Evagelinou, Z. and Weiskopf, M. (1975) Biopolymers 14, 221-226.
23 Hjelm, R.P. and Huang, R.C.C. (1975) Biochemistry 14, 2766-2774.
24 Wilhelm, F.X., de Murcia, G.M., Champagne, H.M. and Daune, M.P. (1974) Eur. J. Biochem. 45, 431-443.
25 Usatyi, A.F. and Shylakhtenko, L.S. (1973) Biopolymers 12, 45-51.
26 Baker, C.C. and Isenberg, I. (1976) Biochemistry 15, 629-634.
27 Greenfield, N.J. and Fasman, G.D. (1969) Biochemistry 8, 4108-4116.
28 Chen, Y.-H., Yang, J.T. and Chau, K.H. (1974) Biochemistry 13, 3350-3359.
29 Breslauer, K.J., Sturtevant, J.M and Tinoco, I., Jr. (1975) J. Mol. Biol. 99, 549-565.
30 Subirana, J.A. (1973) J. Mol. Biol. 74, 363-386.
31 Sahasrabuddhe, C.G. and Van Holde, K.E. (1974) J. Biol. Chem. 249, 152-156.

32 Whitlock, J.P. and Simpson, R.T. (1976) Nucleic Acids Res. 3, 2255-2266.
33 Hanlon, S., Johnson, R.S. and Chan, A. (1974) Biochemistry 13, 3972-3981.
34 Whitlock, J.P. and Simpson, R.T. (1977) J. Biol. Chem. 252, 6516-6520.
35 Bradbury, E.M. and Rattle, H.W.E. (1972) Eur. J. Biochem. 27, 270-281.
36 Li, H.J. (1972) Biopolymers 11, 835-847.
37 Lilley, D.M.J., Howarth, O.W., Clark, V.M., Pardon, J.F. and Richards, B.M. (1974) Biochemistry 14, 4590-4600.
38 Thomas, G.J., Jr., Prescott, B. and Olins, D.E. (1977) Science 197, 385-388.
39 Moss, T., Cary, P.D., Crane-Robinson, C. and Bradbury, E.M. (1976) Biochemistry 15, 2261-2267.
40 Moss, T., Cary, P.D., Abercrombie, B.D., Crane-Robinson, C. and Bradbury, E.M. (1976) Eur. J. Biochem. 71, 337-350.
41 Ackermann, T. (1969) in Biochemical Microcalorimetry (H.D. Brown ed.), Academic Press, New York, p. 131.
42 Privalov, P.L., Ptytsin, O.B. and Birshtein, T.M. (1969) Biopolymers 8, 559-571.
43 Oliver, A.L., Wartell, R.M. and Ratliff, R.L. (1977) Biopolymers 16, 1115-1138.
44 Bloomfield, V.A., Crothers, D.M. and Tinoco, I., Jr. (1974) in Physical chemistry of nucleic acids, Harper and Row, New York, p. 315.
45 Klump, H. (1976) Biophys. Chem. 5, 363-367.
46 McGhee, J.D. and von Hippel, P.H. (1974) J. Mol. Biol. 86, 469-489.
47 McGhee, J.D. (1976) Biopolymers 15, 1345-1375.